ISBN: 978-3-95450-248-6 ISSN: 2673-5490 doi: 10.18429/JACoW-IPAC2025-THPM063

EXTENDED PHASE SPACE TOMOGRAPHY FOR EOSD SIMULATION CONSIDERING CRYSTAL GEOMETRY EFFECTS

F. Donoso*, M. Reissig, S. Funkner, E. Bründermann, M. Frank, A.-S. Müller
Karlsruhe Institute of Technology, Karlsruhe, Germany

Abstract

This theoretical study presents an advanced method for longitudinal phase space tomography in electron storage rings, focusing on reconstructing phase space densities from electro-optical spectral decoding (EOSD) measurements that incorporate crystal geometry effects. The EOSD crystal geometry significantly impacts the measurement signal due to signal integration along its length and interference from wake fields and Cherenkov diffraction radiation (ChDR). These effects add challenges to reconstructing the original phase space density from experimental data.

To address these challenges, we integrate two theoretical frameworks. First, we employ the Vlasov-Fokker-Planck equation to model the turn-by-turn evolution of the charge density distribution. Second, CST simulations of the bunch profile characterize the electric field inside the crystal, enabling a tailored simulation for the EOSD system at the Karlsruhe Research Accelerator (KARA). By combining these approaches, we propose a refined tomography method that more accurately reconstructs the longitudinal phase space from sensor data, effectively capturing the interplay between bunch dynamics and the EOSD system configuration.

INTRODUCTION

This works builds on a prior publication to IPAC 2024 [1], and incorporates the work on modeling the Electro-Optical Spectral Decoding (EOSD) beam diagnostic system installed at KARA [2, 3].

In our previous work [1], we demonstrated that the longitudinal phase space of an electron bunch can be reconstructed from a sequence of simulated bunch profiles by solving a PDE-constrained inverse optimization problem [4], governed by the Vlasov-Fokker-Planck Equation (VFPE) [5].

Equation (1) presents the problem statement, where the goal is to reconstruct the initial phase space distribution by minimizing the difference between measured bunch profiles, $\bar{\rho}_n$, and the corresponding phase space projections, $\rho(q, t_n)$. The objective function is defined as the total distance between the measured charge profiles and the respective projections from the evolving phase space density [1], where $\rho(q, t_n)$ depends of the phase space, making this equation non-linear. The term $\lambda R(\psi)$ is the regularization parameter.

$$\begin{aligned} \min_{\psi^*} \quad & \sum_{n=1}^{m} \|\rho(q,t_n) - \bar{\rho}_n\|^2 + \lambda R(\psi), \\ \text{s.t.} \quad & \frac{\partial \psi}{\partial t} + \frac{\partial H}{\partial p}\frac{\partial \psi}{\partial q} - \frac{\partial H}{\partial q}\frac{\partial \psi}{\partial p} = \beta_d \frac{\partial}{\partial p}(p\psi) + D\frac{\partial^2 \psi}{\partial p^2}, \\ & \rho(q,t) = \int \psi(q,p,t)\mathrm{d}p, \\ & \psi^* = \psi(q,p,t_1). \end{aligned} \tag{1}$$

To solve Eq. (1), we adopt the method presented in the work [6], which solves the VFPE using operator splitting [7] on a discrete spatial grid with time steps corresponding to single-turn revolutions of the bunch in the synchrotron. We have shown that the phase space time evolution can be effectively described as a sequence of matrix operations applied to the current phase space distribution, $\psi(s, t)$, where s denotes the index of the phase space expressed as a one-dimensional vector [1], as illustrated in Eq. (2):

$$\psi(s, t + \Delta t) = \mathrm{D} \cdot \mathrm{R_K} \cdot \mathrm{R_D} \cdot \mathrm{K}(\psi(s,t)) \cdot \psi(s,t). \tag{2}$$

The operators in Eq. (2) represent distinct physical effects over one turn. The "rotation" operators ($\mathrm{R_K}$ and $\mathrm{R_D}$) arise from the *external fields* of the the Hamiltonian, H, while the "damping and diffusion" operator (D) originates from the Fokker-Planck terms describing synchrotron radiation effects. The "wake potential" operator (K) models *collective effects* that depend on the bunch profile, which is determined by the phase space distribution. This dependence introduces nonlinearity into the VFPE, where forces generated by the bunch distribution act back to change their distribution. For details, refer to Refs. [1, 6, 8].

We found that the optimization problem in Eq. (1) can be presented in a discrete expression as in Eq. (3). The dynamic part of the system matrix, $\tilde{\mathrm{W}}$, is constructed turn-by-turn as bunch profile measurements arrive. The target phase space density is represented as a vector ψ, and $\boldsymbol{\rho}$ contains the measured bunch profiles in vector form:

$$\begin{aligned} \min_{\psi} \quad & \|\tilde{\mathrm{W}}\psi - \boldsymbol{\rho}\|^2 + \lambda R(\psi), \\ \text{s.t.} \quad & \mathrm{M}(\psi(s,t_k)) = \mathrm{D} \cdot \mathrm{R_K} \cdot \mathrm{R_D} \cdot \mathrm{K}(\psi(s,t_k)), \\ & \tilde{\mathrm{W}} = \begin{pmatrix} \mathrm{W} \\ \mathrm{W} \cdot \mathrm{M}(\psi(s,t_1)) \\ \vdots \\ \mathrm{W} \cdot \Pi_{k=1}^{n-1} \mathrm{M}(\psi(s,t_k)) \end{pmatrix}. \end{aligned} \tag{3}$$

To solve Eq. (3), we assume that the bunch charge distribution can be directly measured. However, this assumption

* felipe.donoso@kit.edu

ISBN: 978-3-95450-248-6 ISSN: 2673-5490 doi: 10.18429/JACoW-IPAC2025-THPM063

does not hold in the case of EOSD, where the measurable signal is not the bunch profile itself but a phase modulation signal, Γ, induced by electric fields that modify the refractive index of the electro-optical crystal. This alters the phase of a chirped laser pulse as it passes through the crystal [9, 10] due to the Pockels effect [11].

To simulate the EOSD signal, we build upon the simulation approach developed by M. Reißig [3]. In this framework, the electric field generated by the electron bunch inside the crystal is simulated using the Wakefield Solver in CST Studio Suite® [12], which employs a Time Domain Solver. The geometry of the setup is simplified to a 3D model of the vacuum chamber section containing the EO crystal and its holder. The electric fields are sampled along a line through the center of the crystal using virtual probe points.

The phase shift, or retardation, is calculated by summing the contributions of the vertical electric field component, $E_i^{(y)}$, sampled at discrete probe points [3, 9, 10], and applied in Eq. (4).

$$\Gamma \approx \sum_i^n \frac{2\pi d_i}{\lambda} n_0^3 r_{41} E_i^{(y)}(t_i), \tag{4}$$

where d_i is the spacing between consecutive probe points, λ is the central wavelength of the laser, n_0 is the refractive index of the crystal, and r_{41} is its electro-optic coefficient.

This simulation pipeline enables modeling of the EOSD signal formation and allows us to map the bunch profile to the expected phase modulation signal with high temporal fidelity.

In order to use the EOSD simulation the inverse problem is expanded to minimize the difference between the computed phase retardation $\Gamma(t_n)$ and the measured signal $\bar{\Gamma}_n$, as shown in Eq. (5), where G is the operator that maps the bunch profile to the phase retardation:

$$\begin{aligned}
\min_{\psi^*} \quad & \sum_{n=1}^{m} \|\Gamma(t_n) - \bar{\Gamma}_n\|^2 + \lambda R(\psi), \\
\text{s.t.} \quad & \frac{\partial \psi}{\partial t} + \frac{\partial H}{\partial p}\frac{\partial \psi}{\partial q} - \frac{\partial H}{\partial q}\frac{\partial \psi}{\partial p} = \beta_d \frac{\partial}{\partial p}(p\psi) + D\frac{\partial^2 \psi}{\partial p^2}, \\
& \rho(q,t) = \int \psi(q,p,t)\mathrm{d}p, \\
& \Gamma(t_n) = G\left(\rho(q,t_n)\right), \\
& \psi^* = \psi(q,p,t_1).
\end{aligned} \tag{5}$$

SIMULATION OF MEASUREMENTS IN NON-EQUILIBRIUM DYNAMICS

EOSD is a powerful technique for measuring the longitudinal profile of electron bunches with sub-picosecond resolution [13, 14]. To simulate EOSD measurements in non-equilibrium beam dynamics, we combine electric field simulations from CST Studio with Inovesa-generated bunch profiles to compute the phase modulation.

Inovesa is our in-house VFPE solver [8]. The solver generates time-resolved phase spaces and corresponding bunch profiles governed by the VFPE, capturing effects like microbunching [15]. The profiles are used as input in CST's Wakefield Solver to compute the electric fields inside the electro-optical (EO) crystal. The 3D geometry used in the simulation determines the electromagnetic response of the system, constraining the electric fields used to compute the phase retardation of a chirped laser pulse, as shown in Eq. (4).

This approach models EOSD signals by capturing the dynamic evolution of electron bunch profiles and distortions from environmental effects like reflections, Cherenkov refraction, and dispersion. While the full 3D simulation is detailed and physically accurate, it is *resource-intensive*, requiring full electromagnetic calculations for each iteration, and *non-differentiable*, limiting its compatibility with inverse modeling.

To address these limitations, we propose an alternative forward model based on the EOSD system's *impulse response*, leveraging the linearity of Maxwell's equations to treat it as a Linear Time-Invariant (LTI) system [16], with the impulse response defined by the phase retardation from a delta-like charge distribution.

Once the impulse response $h(t)$ is known, see Fig. 1, the corresponding EOSD signal $\Gamma(t)$ for any given bunch profile $\rho(t)$ can be efficiently obtained through convolution:

$$\Gamma(t) = (h * \rho)(t) = \int_{-\infty}^{\infty} h(\tau)\,\rho(t-\tau)\,d\tau. \tag{6}$$

Since CST cannot simulate an ideal delta excitation, we use a Gaussian pulse smaller than the maximum frequency on the simulation. The impulse response is doubled in duration and centered, ensuring each point in the recovered EOSD signal is influenced by the full laser window.

Figure 2 shows that the EOSD signals generated by convolving the bunch profile with the impulse response closely match those obtained from CST simulations.

This convolution-based method offers a practical, accurate and consistent surrogate model for integrating EOSD measurements into inverse problems, while reducing computational overhead.

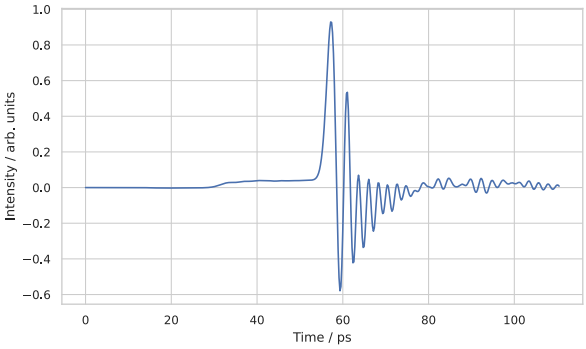

Figure 1: Impulse response of a Gaussian excitation with a temporal width of $\sigma = 0.12$ ps.

ISBN: 978-3-95450-248-6 ISSN: 2673-5490 doi: 10.18429/JACoW-IPAC2025-THPM063

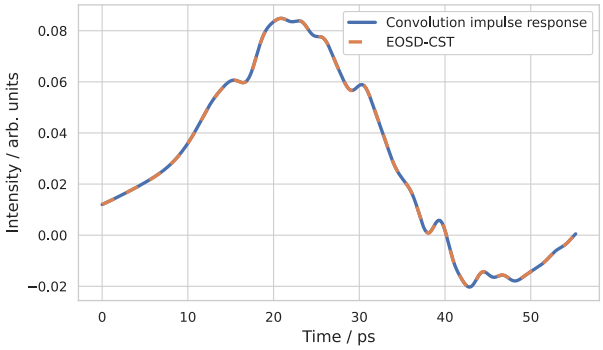

Figure 2: Comparison of EOSD signal from CST simulation and impulse response convolution.

THE EXTENDED PHASE SPACE ALGORITHM

In this work, the relationship between the bunch profile and the resulting phase retardation is modeled by the operator G, defined as the convolution of the system's impulse response with the bunch profile. Within our matrix-based framework, this convolution is formulated as a matrix-vector product, where G is represented by a Toeplitz matrix constructed from the impulse response. This representation provides a structured and computationally efficient means of incorporating the convolution into the inverse problem [17].

$$\Gamma = G \cdot \rho. \tag{7}$$

Therefore, our novel solution can now be written as:

$$\begin{aligned} \min_{\psi} \quad & \|\tilde{G}\psi - \mathbf{\Gamma}\|^2 + \lambda R(\psi), \\ \text{s.t.} \quad & \mathrm{M}(\psi(s,t_k)) = \mathrm{D}\cdot\mathrm{R_K}\cdot\mathrm{R_D}\cdot\mathrm{K}(\psi(s,t_k)), \\ & \tilde{G} = \begin{pmatrix} G\cdot\mathrm{W} \\ G\cdot\mathrm{W}\cdot\mathrm{M}(\psi(s,t_1)) \\ \vdots \\ G\cdot\mathrm{W}\cdot\Pi_{k=1}^{n-1}\mathrm{M}(\psi(s,t_k)) \end{pmatrix}. \end{aligned} \tag{8}$$

The matrix M depends directly on the bunch profile, which is unknown. We cannot deconvolve each EOSD measurement to retrieve the bunch profile, while deconvolution works perfectly for an ideal convolution, even minor discrepancies, or the presence of noise, bias, and model mismatches makes a one-shot deconvolution method ineffective.

To address this issue, we propose an iterative method that begins with a Gaussian approximation of the bunch profile derived from a fit to the measured EOSD signal. This initial profile is then used to compute the matrix M, and subsequently the matrix $\tilde{G}$. The matrix $\tilde{G}$ is constructed similarly to $\tilde{W}$ but with the Toeplitz matrix appended at the end. The phase space obtained from this minimization is subsequently used to calculate new bunch profiles via the matrix $\tilde{W}$. The updated bunch profiles are used to recompute M and solve Eq. (8). In practice, we found that two iterations of the algorithm, see Fig. 3, are enough to convergence.

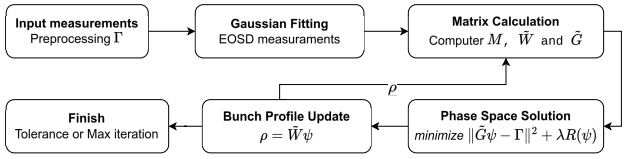

Figure 3: Extended Phase space tomography algorithm.

RESULTS

Figure 4 shows the comparison between the target phase space and the reconstruction from our tomography algorithm. The target phase space was generated from Inovesa with a beam energy of 1.285 GeV and a bunch current of 0.85 mA, which is typical KARA operations. A total of 164 EOSD measurement simulations, corresponding to half a synchrotron period, were used for the reconstruction.

The reconstructed phase space successfully reproduces all prominent micro-bunching structures and matches the target intensity distribution. The reconstruction was performed using two iterations of the extended tomography algorithm shown in Fig. 3. The MATLAB-based implementation, without runtime optimization, required approximately eight hours to complete.

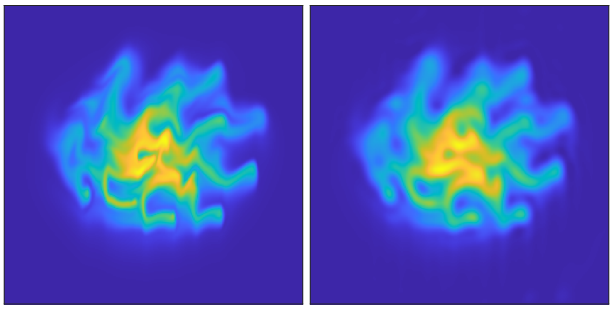

(a) (b)

Figure 4: (a) Target, and (b) Reconstructed phase space.

CONCLUSION

The use of the EOSD system's impulse response to approximate measurements via convolution has proven effective in simulation scenarios, accurately reconstructing the expected signals. The next steps will focus on validating the robustness of the algorithm by testing under different dynamical conditions, adding noise and bias, and eventually applying it to real EOSD data. Additionally, the algorithm will be re-implemented in C++, including CPU parallelism and GPU acceleration, to improve the computational performance.

ACKNOWLEDGEMENTS

F. D. gratefully acknowledge support from the MathSEE PhD Bridge Program at KIT and KCDS.

ISBN: 978-3-95450-248-6 ISSN: 2673-5490 doi: 10.18429/JACoW-IPAC2025-THPM063

REFERENCES

[1] F. Donoso *et al.*, "Longitudinal phase space density tomography constrained by the Vlasov-Fokker-Planck equation", in *Proc. IPAC'24*, Nashville, TN, USA, pp. 2350–2353, 2024. doi:10.18429/JACoW-IPAC2024-WEPG55

[2] M. Reissig *et al.*, "Development of an electro-optical longitudinal bunch profile monitor at KARA towards a beam diagnostics tool for FCC-ee", in *Proc. IPAC'22*, Bangkok, Thailand, pp. 296–299, 2022. doi:10.18429/JACoW-IPAC2022-MOPOPT025

[3] M. Reissig *et al.*, "Simulations of an electro-optical in-vacuum bunch profile monitor and measurements at KARA for use in the FCC-ee", in *Proc. IPAC'24*, Nashville, TN, USA, pp. 2354–2357, 2024. doi:10.18429/JACoW-IPAC2024-WEPG56

[4] M. Hinze *et al.*, *Optimization with PDE Constraints*. Springer, 2009, 270 pp. doi:10.1007/978-1-4020-8839-1

[5] H. Wiedemann, *Particle Accelerator Physics*. Springer Cham, 2015. doi:10.1007/978-3-319-18317-6

[6] R. Warnock *et al.*, "A general method for propagation of the phase space distribution, with application to the Sawtooth instability", SLAC, Stanford, CA, USA, Tech. Rep. SLAC-PUB-8404, 2000. doi:10.2172/753322

[7] E. Sonnendrücker *et al.*, "The semi-Lagrangian method for the numerical resolution of the Vlasov equation", *J. Comput. Phys.*, vol. 149, no. 2, pp. 201–220, 1999. doi:10.1006/jcph.1998.6148

[8] P. Schönfeldt *et al.*, "Parallelized Vlasov-Fokker-Planck solver for desktop personal computers", *Phys. Rev. Accel. Beams*, vol. 20, no. 3, p. 030 704, 2017. doi:10.1103/PhysRevAccelBeams.20.030704

[9] B. Steffen, "Electro-optic methods for longitudinal bunch diagnostics at FLASH", Ph.D. dissertation, University of Hamburg, 2007.

[10] S. Casalbuoni *et al.*, "Numerical studies on the electro-optic detection of femtosecond electron bunches", *Phys. Rev. ST Accel. Beams*, vol. 11, no. 7, p. 072 802, 2008. doi:10.1103/PhysRevSTAB.11.072802

[11] H. Eugene, *Optics*, 4th int. ed. Addison-Wesley, 2002.

[12] *CST Studio Suite*, Dassault Systems, 2024. https://www.3ds.com/products/simulia/cst-studio-suite

[13] B. Steffen *et al.*, "Electro-optic time profile monitors for femtosecond electron bunches at the soft x-ray free-electron laser FLASH", *Phys. Rev. ST Accel. Beams*, vol. 12, no. 3, p. 032 802, 2009. doi:10.1103/PhysRevSTAB.12.032802

[14] S. Funkner *et al.*, "High throughput data streaming of individual longitudinal electron bunch profiles", *Phys. Rev. Accel. Beams*, vol. 22, no. 2, p. 022 801, 2019. doi:10.1103/PhysRevAccelBeams.22.022801

[15] M. Brosi, "In-depth analysis of the micro-bunching characteristics in single and multi-bunch operation at KARA", Karlsruher Institut für Technologie, Karlsruhe, Germany, 2020.

[16] A. Oppenheim *et al.*, *Signals & Systems*, 2nd ed. Prentice Hall, 1997.

[17] P. Hansen, "Deconvolution and regularization with Toeplitz matrices", *Numerical Algorithms*, vol. 29, no. 4, pp. 323–378, 2002. doi:10.1023/A:1015222829062